INFLUENCE OF PROBE LOSSES ON THE ION DENSITY OF A THERMAL ALKALI PLASMA IN A MAGNETIC FIELD

E. Guilino and M. Hashmi [+])

IPP 2/38 June 1965

INSTITUT FÜR PLASMAPHYSIK

GARCHING BEI MÜNCHEN

INSTITUT FÜR PLASMAPHYSIK

GARCHING BEI MÜNCHEN

INFLUENCE OF PROBE LOSSES ON THE ION DENSITY OF A THERMAL ALKALI PLASMA IN A MAGNETIC FIELD

E. Guilino and M. Hashmi [+])

IPP 2/38 June 1965

[+]) Max-Planck-Institut für Physik und Astrophysik, München.

Die nachstehende Arbeit wurde im Rahmen des Vertrages zwischen dem Institut für Plasmaphysik GmbH und der Europäischen Atomgemeinschaft über die Zusammenarbeit auf dem Gebiete der Plasmaphysik durchgeführt.

IPP 2/38

E. Guilino
M. Hashmi

Influence of Probe Losses on the Ion Density of Thermal Alkali Plasma in a Magnetic Field, June, 1965 (in English).

ABSTRACT

According to the "Equilibrium Theory" the ion density on the axis of a thermal alkali plasma in a strong magnetic field should be mainly determined by the end plate losses and hence described by the SAHA equation.

However, measurements of the ion density with Langmuir single probes in a cesium plasma have shown discrepancies up to more than one order of magnitude, depending on density and plate temperature. A modification of the "Equilibrium Theory" is described which takes into account the particle losses at the probe surface. The calculations yield agreement with the experiments.

1. Introduction

The experiments on diffusion of plasma across a magnetic field [1] in a Q-machine by D'ANGELO and RYNN [2] indicated that the recombination coefficient in an alkali plasma was one to two orders of magnitude larger than expected from two- and three-body recombination. This has been later explained by v.GÖLER [3] to be due to the recombination of ions on the hot end plates. According to the 'equilibrium theory' of v.GÖLER the ion density on the axis of a thermal alkali plasma in a strong magnetic field should be mainly determined by the end plate losses and hence described by the SAHA equation. Several experiment have been performed to test this model.

The experiments on ALMA II by ECKHARTT et al. [4], using Langmuir probes to measure the density, yielded loss rates much larger than predicted by the 'equilibrium theory', especially in the low-density range. MOTLEY [5] obtained identical results on Q-3 using the same probe techniques. D'ANGELO and v.GÖLER [6] attributed the observed discrepancy to ion losses at the Langmuir probes and succeeded in showing experimentally the effect of probe loss on the ion density by taking probes of different sizes. But they could explain the above mentioned discrepancy only qualitatively.

The influence of the current collected by the probe on the measureddensity, however, had already been pointed out by KNECHTLI and WADA [7].

The present paper discusses the perturbation of plasma by a probe and results in a modification of the 'equilibrium theory'. The calculations agree with the experiments.

2. Theory

In a magnetic field a Langmuir probe will draw current from a 'tube' of plasma whose cross section (perpendicular to the magnetic field) be A_c. Due to the additional ion losses at the probe surface of area A_p there will be a density depression in the perturbed surroundings, while the density beyond this region will remain nearly unaltered. The classical diffusion perpendicular to the magnetic field as well as the diffusion at the end plates [9] will, in general, contribute to the flux into the perturbed region. These effects as well as the volume recombination can be neglected as shown in appendix 2 and reference 3). Moreover, thermal equilibrium will be assumed, i.e. $T_e = T_i = T_p$, where T_e, T_i, and T_p are the electron, ion, and end plate temperatures, respectively. In order to evaluate the extent of probe perturbation the balance equations can be written for the 'tube' of plasma of cross section A_c, producing the probe current and bounded axially by the two hot end plates.

Volume balance of ions:

$$2j_i A_c = \frac{2}{4} n v_i A_c p_2 + \frac{1}{4} n v_i A_p \quad , \tag{1}$$

volume balance of electrons:

$$2j_e A_c = \frac{2}{4} n v_e A_c p_1 \quad , \tag{2}$$

wall balance of cesium particles:

$$2j_i + 2j_g = \frac{2}{4} n v_i p_2 + j_o \quad , \tag{3}$$

Richardson-Dushmann equation:

$$j_e = Ri(T)\, p_2 \quad , \tag{4}$$

Langmuir-Saha equation:

$$j_i = La(T)\, p_1 j_g \quad ; \tag{5}$$

where:

j_i, j_e, and j_g = current density of ions, electrons, and neutral cesium atoms, respectively, coming from the end plates into the plasma $[cm^{-2}sec^{-1}]$;

j_o = current density of the cesium atomic beam striking the hot end plates $[cm^{-2}sec^{-1}]$;

v_i and v_e = mean thermal velocities of ions and electrons, respectively $[cmsec^{-1}]$;

n = density in the perturbed 'tube' of plasma $[cm^{-3}]$;

$Ri(T)$ = $AT^2 \exp(-e\Phi/kT)$
($A = 4\pi em(k^2/h^3) = 120$ amp/cm^2($^oK^2$),
$\Phi = 4.53$ ev for W
and
4.35 ev for Ta [8]);

$La(T)$ = $(g_+/g_o) \exp(e(\Phi-I)/kT)$
($I = 3.89$ ev for Cs, g_+ and g_o are the quantum mechanical weight factors);

p_1 and p_2 = probability of a charged particle to overcome the sheath voltage U_s,

$$\left.\begin{array}{lll} p_1 = \exp(eU_s/kT), & \text{if } U_s < 0, & \\ \quad = 1 \quad\quad\quad , & \text{if } U_s \geqslant 0, & \\ p_2 = \exp(-eU_s/kT), & \text{if } U_s > 0, & \\ \quad = 1 \quad\quad\quad , & \text{if } U_s \leqslant 0; & \end{array}\right\} \qquad (6)$$

A_p = effective probe area.

Eq. (2) is valid as long as the electron current to the probe is negligible compared to the electron current to the end plates, i.e.:

$$2p_1 \frac{A_c}{A_p} \frac{v_e}{v_i} \gg 1$$

which is generally fulfilled in all the experiments except when the probe draws electron current.

Eqs. (1) to (6) yield:

1) In the presence of an electron sheath:

$$p_1 = 1 \; ; \qquad p_2 = nv_e/4Ri \; ;$$

$$j_o = \frac{1}{4} nv_i \left[\frac{2n}{Sa(T)} + \frac{A_p}{A_c} \frac{La+1}{La} \right] \; ; \qquad (7)$$

2) in the presence of an ion sheath:

$$p_1 = 4R_i/nv_e \; ; \qquad p_2 = 1 \; ;$$

$$j_o = \frac{1}{4} nv_i \left[\frac{2n}{Sa(T)} \left(1 + \frac{1}{2} \frac{A_p}{A_c}\right) + \frac{A_p}{A_c} \right] \; ; \qquad (8)$$

where:

$$Sa(T) = \left(\frac{2g_+}{g_o}\right)\left(\frac{2\pi m_e kT}{h^2}\right)^{3/2} \exp\left(\frac{-eI}{kT}\right) \; ,$$

$$= \left(\frac{4}{v_e}\right) Ri(T) \; La(T) \; .$$

If there is no sheath at the end plates ($p_1 = p_2 = 1$), Eqs. (7) and (8) become identical. Neglecting the influence of the probe ($A_p/A_c = 0$) Eqs. (7) and (8) become identical with the results of reference 3).

Determination of A_p/A_c

The quantity A_p/A_c is required to determine the probe losses in Eqs. (7) and (8).

For a sufficiently large plasma diameter, the region of influence of probe perturbation will be a function of the gyration radius of the ions. One would expect that the probe will draw current only from a 'tube' of plasma whose cross section A_c is formed by all points less than twice the radius of gyration from the edge of the probe tip in a plane perpendicular to the magnetic field. If the radius of gyration becomes comparable to or exceeds the radius of the plasma column, A_c may be replaced by the cross section of the plasma column.

Remembering that radial mass flow by diffusion is neglected and the experimental density profiles are replaced by a constant density within the 'tube' of plasma, the diameter of the 'tube' has to be reduced to an effective value in order to obtain the same current to the probe (see Fig. 1). Under these conditions, as will be shown in a forthcoming report, in case of a non-rotating column and probe situated at the center, the current to the probe will flow from a 'tube' of plasma of cross section A_c which is limited in all directions in a plane $\perp \underline{B}$ by $1.5\, r_{ci}$ from the edge of the probe tip, as shown in Fig. 2 . If the plasma column is rotating, A_c is given by the rotation of the above mentioned figure about the axis of the column, as represented in Fig. 3 . Provided that the probe is situated at the axis, A_c is represented by the area of a circle having a radius $r_c = \{1.5\, r_{ci}$ + the largest distance between the edge of the probe tip and the axis of rotation$\}$. In this case the effect of rotation on A_c is quite small. The present paper deals only with probes on the axis of the plasma column. The increase in the effective probe area due to the surrounding sheath should be considered only for very small probes and densities below 10^9 cm^{-3}, otherwise it is negligible.

A_c is obtained from Figs. 2 and 3 as follows:

1) Non-rotating plasma; probe on the axis:

a) cylindrical probe:

$$A_c = 2\rho\ell + 2 \times 1.5 r_{ci} \ell + 2 \times 1.5 r_{ci} 2\rho + 4\tfrac{1}{4}\pi\,(1.5 r_{ci})^2 ,$$

$$= 2\rho\ell + 3 r_{ci}\,(2\rho + \ell + \pi r_{ci}) ; \qquad (9)$$

b) plane probe $\perp \underline{B}$:

$$A_c \approx \pi\,(\rho + 1.5 r_{ci})^2 . \qquad (10)$$

2) Rotating plasma; probe on the axis:

a) cylindrical probe:

$$A_c = \pi\,(\tfrac{\ell}{2} + 1.5 r_{ci})^2 ; \qquad (11)$$

b) plane probe $\perp \underline{B}$:
see Eq. (10).

Not only the metallic tip but also the insulator of the probe will collect ions from A_c. The latter assumes floating potential; this is equivalent to the flow of ion saturation current. Morevoer, the area of the probe $\parallel \underline{B}$ should also be considered. It would collect ions as long as its dimensions $\parallel \underline{B}$ are smaller than the pitch h of the gyrating spiral:

$$h \approx \frac{v_i}{\nu_{ci}} = 1.09 \times 10^2 \frac{\sqrt{T}}{B} \quad [T \text{ in } {}^{o}K;\ B \text{ in } \Gamma;\ h \text{ in cm}] .$$

If $T_p > 1970\,{}^{o}K$ and $B < 10^4\ \Gamma$, which condition is fulfilled by the experiments described here, one obtains:

$$h \geqslant 0.5 \text{ cm} ;$$

on the other hand, the largest probe had a diameter of 4.7 mm.

Therefore, one does not need to distinguish between parts of the probe parallel and perpendicular to $\underline{B}$. A_p is the total area of the probe immersed in the 'tube' of plasma of cross section A_c; for instance, for a cylindrical probe on the axis of a non-rotating plasma column, A_p will be:

$$A_p = 2\pi\rho\ell + \frac{\pi}{4} d_{ins}^2 + 2\pi \frac{d_{ins}}{2} 1.5\, r_{ci} ,$$

$$= \pi \left(2\ell\rho + \frac{d_{ins}^2}{4} + 1.5\, r_{ci}\, d_{ins}\right) .$$

Thus, it is possible to evaluate A_p/A_c for various probe sizes, magnetic fields, and plate temperatures.

It should be mentioned here that D'ANGELO and v.GÖLER have empricially determined A_p/A_c by the relation:

$$n = \frac{A_c}{A_p} \frac{4\Phi_o}{v_i} . \qquad (12)$$

Keeping the total input flux constant (Φ_o = 0.1 mA), they measured the density at different plate temperatures and obtained:

$$\frac{A_p}{A_c} = 0.27 .$$

Obviously, this value of A_p/A_c is valid only for a particular probe size and magnetic field. Moreover, Eq. (12) attributes,

by definition, all possible losses to the probe except those at the end plates.

The outcome of the present theory is twofold: Firstly, it predicts A_c. Microwaves measure the mean density of the plasma cross section and hence are not sensitive enough to indicate any local density depression. Barium plasmas, on the other hand, exploiting the resonance scattering of photons by Ba ions, are well suited to verify A_c. Such an experiment is already underway. Secondly, the theory describes a relation between the total input flux and the density (Eqs. 7 and 8), which can be compared with the experimental results already available. This will be the subject of the present paper.

3. Comparison of theory with experiments

3.1. Measurement of the neutral current density j_o

A relation between the peak density n and the neutral current density j_o is given by Eqs. (7) and (8). The experiments, however, do not determine the neutral flux density j_o, but the ion saturation current to a tantalum plate inserted temporarily into the plasma. The diameter of the tantalum plate was twice to that of the plasma column. j_o must now be evaluated from the measured current i_m.

To determine the ion current density, $\Phi_m = i_m/F_{eff}$, the measured radial density profile is replaced by a rectangular one; both having the same peak density n_o, i.e.:

$$n_o F_{eff} 2 l_o = \int_V n' dV = N \quad \text{and} \quad r_{eff}^2 = \frac{F_{eff}}{\pi} , \tag{13}$$

where: $2 l_o$ = distance between the end plates,
n' = density in the volume element dV,
N = total number of ions in the plasma column.

For ALMA II, $2r_{eff}$ was found to be 3 cm; and for Q-3: 1.7 cm [10].

The relation between Φ_m and j_o for an ion sheath has been derived in reference 6). Considering the electron sheath as well, one obtains:

$$\frac{j_o}{\Phi_m} = 1 + \frac{1+p_2}{p_1} \frac{1-\gamma}{\gamma} ,$$

where:

$$\gamma = \frac{1}{1 + \frac{g_o}{g_+} \exp((I-\Phi)/kT)}$$

γ represents the probability of ionization of a particle, neutral or ion, at the end plate; $g_o/g_+ = 2$.

Now:

- In presence of an ion sheath:

$$p_2 = 1 \quad ; \qquad 0 < p_1 < 1 \quad ;$$

$$\frac{j_o}{\Phi_m} = 1 + \frac{2}{p_1} \frac{1-\gamma}{\gamma} \quad ; \tag{14}$$

$$p_1 \to 0 \quad : \qquad \frac{j_o}{\Phi_m} \to \infty \quad .$$

- In presence of an electron sheath:

$$p_1 = 1 \quad ; \qquad 0 < p_2 < 1 \quad ;$$

$$\frac{j_o}{\Phi_m} = 1 + (1+p_2) \frac{1-\gamma}{\gamma} \quad ; \tag{15}$$

$$p_2 \to 0 \quad : \qquad \frac{j_o}{\Phi_m} \to \frac{1}{\gamma} \quad . \tag{15a}$$

- If there is no sheath:

$$p_1 = p_2 = 1 \quad ;$$

$$\frac{j_o}{\Phi_m} = 1 + 2 \frac{1-\gamma}{\gamma} \quad . \tag{16}$$

j_o/Φ_m as a function of p_1/p_2 (Eq. 2) is shown in Fig. 4.

3.2. MOTLEY's experiment at Q-3 in Princeton

n versus i_m curves for T_p = 2500, 2360, 2180, and 1970 °K at a magnetic field of 10 kΓ were measured. A cylindrical probe having a diameter of the metallic tip $2\rho = 0.38$, length of the metallic tip $\ell = 0.76$ mm, and diameter of the insulator $d_{ins} = 1.4$ mm was used.

Table 1 represents A_p/A_c for this probe.

Table 1

T_p	2500	2360	2180	1970	^oK
r_{ci}	0.75	0.73	0.70	0.66	mm
A_c	7.1	6.8	6.45	5.2	mm^2
A_p/A_c	1.05	1.07	1.1	1.14	

According to Eq. (14), in presence of an ion sheath, n should be proportional to Φ_m. Both the Q-3 experiments, however, exhibit a clear $n \sim \Phi_m^2$ dependence in presence of an ion sheath. Accordingly, agreement with the present theory is attained only, if j_o in both Q-3 experiments is determined by means of Eq. (15a) instead of Eq. (14). As the details of the Q-3 experiments are not known to us, an interpretation will not be attempted here. It may have the following reasons:

1) A large withdrawal of ions while measuring the flux could create a strong electron sheath at the end plates.
2) A large pressure gradient $\| \underline{B}$ ($p = 0$ at the tantalum plate) makes sheath effects negligible.

On the contrary, this effect does not appear in ALMA II experiments, where agreement with theory is achieved with j_o determined by Eq. (14).

Figs. 5 to 8 compare theory with experiment. Curve (1) corresponds to the equilibrium model and curve (2) represents the present theory obtained from Eqs. (7) and (8).

Figs. 5 and 6 show good agreement with curve (2). Deviations from the present theory in Figs. (7) and (8) can be attributed to an uncertainty of about 100 ^oK in the pyrometric measurement of the plate temperature which enters exponentially in Eq. (8). Hence, in presence of an ion sheath the term $\frac{2n}{Sa(T)}$ in Eq. (8) is very sensitive to T_p. In presence of an electron sheath, however, the dominating term in Eq. (7) is essentially proportional to $\sqrt{T_p}$. To demonstrate this, we show curves (3) and (4) in Fig. 8, which are calculated by assuming a tempera-

ture higher by 50 °K than of curve (2), whereas curve (2a) in Fig. 5 represents a temperature lower by 50 °K . Therefore, in presence of an ion sheath, the deviations or agreements should not be overstressed because of the uncertainty in T_p. On the other hand, in the presence of an electron sheath, the agreement should not be regarded as accidental.

In some of the measurements, the plasma was surrounded by an iris 2.8 cm in diameter placed at the mid plane and biased negative with respect to the plate. In Figs. 5 to 8 the right end of the horizontal bars represents the total neutral flux density; the left end is the neutral flux density after subtracting the neutral flux density corresponding to the ion current collected by the iris.

3.3. The experiment by D'ANGELO and v.GÖLER at Q-3 in Princeton

n versus Φ_m curves were measured. Three different cylindrical probes (their sizes are given in table 2) were used to determine the density. The magnetic field was 9 kΓ, the temperature of the end plates was 2500 °K. In Figs. 9 to 11 the experiments are compared with theory. Curve (1) corresponds to the 'equilibrium theory', curve (2) represents the present theory. Curve (3) is obtained by taking the empirical value of $A_p/A_c = 0.27$ from Eq. (12) by D'ANGELO and v.GÖLER. In this experiment also j_o was determined by Eq. (15a). The error in measuring T_p was about 100 °K. Curve (2a) shows how a decrease of 50 °K in T_p will modify curve (2). The agreement achieved between experiment and theory up to $A_p/A_c = 2.57$ is good.

T a b l e 2

Probe	"a"	"b"	"c"	
Diameter of the metallic tip, 2ρ	7.6×10^{-2}	0.38	1.27	mm
Length of the metallic tip, ℓ	0.38	0.76	2.03	mm
Diameter of the insulator, d_{ins}	0.76	1.27	4.45	mm
A_c	6.3	8.15	15.9	mm^2
A_p/A_c	0.35	0.87	2.57	

3.4. The experiment with ALMA II at IPP

n and j_o were determined for various plate temperatures between 2100 °K and 2375 °K. However, the temperature of both end plates were not identical during all the runs. The magnetic field was varied between 1.2 and 3.3 kΓ. Two different types of probes were used to measure the density:

1) Cylindrical probe:

diameter of the metallic tip 2ρ = 0.8 mm,
length " " " " ℓ = 2 mm,
diameter " " insulator d_{ins} = 2 mm.

2) Plane probe:

diameter of the metallic surface 2ρ = 3 mm,
diameter " " insulator d_{ins} = 2 mm.

Neglecting the influence of T_p on A_p/A_c one obtains:

Table 3

Probe	cylindrical (1)		plane (2)			
B	2000	2850	1200	2000	3000	gauss
r_{ci}	3.8	2.65	6.1	3.8	2.3	mm
A_c	141	77.5	356	164	77	mm^2
A_p/A_c	0.31	0.43	0.22	0.35	0.52	

In Fig. 12 the experimental value of j_o acquired by means of Eqs. (14), (15), and (16) is compared with the theoretical j_o evaluated from the measurements of n and T_p with the aid of Eqs. (7) and (8). If the experiments agree with theory, all the points should fall on a straight line making a 45° angle with the axes. Deviations have the following reasons:

1) About 2/3 of the points were measured in presence of an ion sheath. Therefore, an error of ± 100 °K in the measurement

of T_p enters exponentially into the calculations as mentioned above. Moreover, measurements were not made under conditions where probe losses were dominating.

2) During the runs, when the temperature of the end plates was not identical, a current $\parallel \underline{B}$ may have flowed. However, this effect has not been considered in the present theory.

In spite of such crude conditions, the mean deviation is:

$$\epsilon = \frac{1}{i} \sum_i \frac{|j_{th} - j_m|}{j_m} \approx 30\ \% \quad .$$

The chief purpose of comparison of theory with this experiment is to show that even at low magnetic fields, where A_c becomes comparable with the plasma cross section, the present theory still adequately describes the particle losses due to the probe.

4. Conclusion

It has been shown that the present theory describes adequately the experiments for $1200 \leqslant B \leqslant 10000$ Γ, $10^{10} \leqslant n \leqslant 3 \times 10^{12}$ cm^{-3}, $1950 \leqslant T_p \leqslant 2500$ °K, and $2.2 \leqslant A_p \leqslant 60$ mm^2. Furthermore, the probe seems to measure correctly the perturbed density prevailing in its surroundings. It appears to be extremely difficult to construct a probe whose perturbing effect can be neglected at low densities and high plate temperatures, as the surface of the insulating supporter immersed into A_c as well as the surface of the probe $\parallel \underline{B}$ must be included in the effective surface of the probe. This is also true for a floating probe. Very thin wire probes extending across the plasma column used by KNECHTLI and WADA are also not suited for lower densities because of the creation of a sheath around them.

Acknowledgement

We wish to thank Drs. G. v.Gierke, G. Grieger, G. Müller, and Mr. H.P. Zehrfeld for valuable comments and discussions.

Appendix 1

A remark on the particle loss rates of a cesium plasma in a curved magnetic field geometry [4].

The experiment of reference 4 was performed to study the behaviour of a cesium plasma in a curved geometry. The density profiles, using probes, were measured as a function of the radius of curvature R_c. A density depression of about a factor 2 was observed by bending the originally homogeneous magnetic lines to a radius of curvature of 2 meters. "Enhanced" stellarator losses in the curved field (which are described by the BOHM-diffusion coefficient within a factor 3), on the contrary, would cause a density depression of a few orders of magnitude if the mean life time τ of the particles in the homogeneous magnetic field were governed by classical diffusion and end plate recombination.

It has been shown in the preceeding sections that due to the ion losses at the probe surface, the mean life time τ of the particles could be enormously diminished in the homogeneous magnetic field. Hence, the decrease in density by curving the magnetic lines should be much smaller even if 'enhanced' losses would appear. This will be estimated in the following.

In the stationary state the total ion input flux $\Phi_i A_c$ is equal to the total loss rate of the particles.

$$\Phi_i A_c \tau = \int_V n' \, dV = N = n2 \, l_o A_c \qquad (17)$$

and, neglecting the classical diffusion:

$$\frac{1}{\tau} = \frac{1}{\tau_\alpha} + \frac{1}{\tau_s} \quad , \qquad (18)$$

where τ_α and τ_s are the mean life times of the particles determined by the recombination at the end plates and at the probe surface, respectively.

$$\tau_\alpha = \frac{1}{\alpha n} \quad ; \quad \tau_s = \frac{8 l_o}{v_i} \frac{A_c}{A_p} \approx 17 \text{ msec} \qquad (19)$$

(α = end plate recombination coefficient [3]; $A_c/A_p = 0.31$ for probe I of section 3.4; B = 1800 Γ).

The results of reference 4 were divided into three groups:

I : $n > 3 \times 10^{11}$ cm^{-3}; T_p(mean) = 2275 °K; B = 1800 Γ;
the density $\bar{n}$ averaged over the whole region = 5×10^{11} cm^{-3}.

II : $10^{11} < n < 3 \times 10^{11}$ cm^{-3}; T_p(mean) = 2200 °K; B = 1800 Γ;
$\bar{n} = 1.5 \times 10^{11}$ cm^{-3}.

III: $n < 10^{11}$ cm^{-3}; T_p(mean) = 2100 °K; B = 1800 Γ;
$\bar{n} = 3 \times 10^{10}$ cm^{-3}.

For homogeneous magnetic fields the mean life times estimated for the above mentioned groups are correct within a factor 2.

Region I : $$\alpha = \frac{1}{l_o} \frac{v_i}{4Sa(T)} \frac{1}{1+1/La(T)\, p_1} \approx 2.7 \times 10^{-10} \text{ cm}^3/\text{sec},$$

$$\tau_\alpha = 3.7 \times 10^9 \frac{1}{n} \text{ sec},$$

$$\tau \approx 5 \text{ msec}.$$

Region II : $$\alpha = \frac{1}{l_o} \frac{v_i}{4Sa(T)} \frac{1}{1+1/La(T)\, p_1} \approx 7 \times 10^{-10} \text{ cm}^3/\text{sec},$$

$$\tau_\alpha = 1.5 \times 10^9 \frac{1}{n} \text{ sec},$$

$$\tau \approx 6.3 \text{ msec}.$$

Region III: $$\alpha \approx \frac{1}{l_o} \frac{v_i}{4Sa(T)} \approx 2.5 \times 10^{-9} \text{ cm}^3/\text{sec},$$

$$\tau_\alpha \approx 4 \times 10^8 \frac{1}{n} \text{ sec},$$

$$\tau \approx 7.3 \text{ msec}.$$

These values are comparable with τ_{Bohm} which is given by:

$$\tau_{Bohm} \approx \frac{r_{eff}^2}{2D_{Bohm}} \; ; \qquad D_{Bohm} = 10^8 \frac{U_{th}}{16B} \; cm^3/sec \; ;$$

$$\tau_{Bohm} \approx 1.6 \; msec \qquad \text{for } B = 1800 \; \Gamma \; .$$

If the flux remains constant:

$$\frac{\tau_R}{\tau} = \frac{n_R}{n} \; , \tag{20}$$

where τ_R and τ are the mean life times in homogeneous and curved magnetic fields, respectively. n_R and n are the corresponding densities.

Considering the equilibrium losses of reference 4 as well,

$$\tau_{equilibrium} = 5 \times 10^9 \frac{1}{n} \; sec \text{ for } R_c \; 2 \; m \text{ and } B = 1.8 \; k\Gamma,$$

one obtains:

$$\frac{1}{\tau_R} = \frac{1}{\tau} + \frac{1}{\tau_{eq}} + \frac{1}{\tau_{Bohm}} \; . \tag{21}$$

One should expect now the following n_R/n, if BOHM diffusion appears (R = 2 m, B = 1.8 kΓ).

Groups I : $n_R/n = 0.21$,
" II : $n_R/n = 0.19$,
" III: $n_R/n = 0.18$.

This clearly shows that, if the density is measured by probes, 'enhanced' losses lead to a density depression n_R/n not of orders of magnitude, but only of a factor 4 to 5. Whether 'enhanced' losses take place cannot be decided from the experimentally observed n_R/n of 0.6 to 0.8.

Appendix 2

The diffusion in the present theory can be neglected, if the flux Φ_D due to diffusion into the perturbed 'tube' of plasma is small compared to the sum of the flux Φ_s to the probe and the flux Φ_α to the end plates, i.e.:

$$\varphi = \frac{\Phi_\alpha + \Phi_s}{\Phi_D} >> 1 \ . \tag{22}$$

The flux Φ and the mean density n are related by:

$$\Phi\tau = n V \ . \tag{23}$$

Therefore,

$$\left.\begin{aligned} \Phi_\alpha &= \frac{nV}{\tau_\alpha} \ , \\ \Phi_s &= \frac{nV}{\tau_s} \ , \\ \Phi_D &= \frac{nV}{\tau_D} \ . \end{aligned}\right\} \tag{24}$$

Combining Eqs. (22) and (24) one obtains:

$$\varphi = \tau_D \left(\frac{1}{\tau_\alpha} + \frac{1}{\tau_s}\right) = \frac{A_c}{2\pi D R} \frac{n}{\nabla n} \left(\frac{1}{\tau_\alpha} + \frac{1}{\tau_s}\right) \ , \tag{25}$$

where

$$\tau_D = \frac{A_c}{2\pi D_{classical} R} \frac{n}{\nabla n} \ , \tag{26}$$

R being the radius of the perturbed 'tube' of plasma.

$$D_{classical} = 1.65 \times 10^{-5} \frac{\ln \Lambda}{\sqrt{U_{th}}} \frac{n}{B^2} \ ;$$

$$\ln \Lambda = 10 \ ;$$

$$\sqrt{U_{th}} = 0.45 \ ;$$

$$D_{classical} = 3.66 \times 10^{-4} \frac{n}{B^2} \ .$$

If the flux Φ_o in the perturbed 'tube' of plasma remains constant over the whole diameter 2R :

$$\frac{\nabla n}{n} \approx \frac{1}{R} \left(\frac{n_a - n_i}{n_a}\right) = \frac{1}{R} \left(1 - \frac{n_i}{n_a}\right) \quad , \tag{27}$$

n_i and n_a being the densities inside and outside the perturbed 'tube' of plasma, respectively.

According to Eq. (23)

$$\frac{n_i}{n_a} = \frac{\tau_i}{\tau_a} \qquad \text{and:} \quad \tau_i = \frac{1}{1/\tau_\alpha + \frac{1}{\tau_s}} \quad ,$$

$$\tau_a = \tau_\alpha \quad .$$

Now: $$\frac{n_i}{n_a} = \frac{1}{\tau_\alpha \left(\frac{1}{\tau_\alpha} + \frac{1}{\tau_s}\right)} = \frac{1}{1 + \frac{\tau_\alpha}{\tau_s}} \quad . \tag{28}$$

Hence, Eq. (27) can be written as:

$$\frac{\nabla n}{n} \approx \frac{1}{R} \left(\frac{\tau_\alpha}{\tau_\alpha + \tau_s}\right) \quad . \tag{29}$$

Substituting D, $\nabla n/n$, τ_α, τ_s, etc. in Eq. (22) one obtains:

$$\varphi = 4.35 \times 10^2 \frac{v_i}{8 l_o} A_p \frac{B^2}{n} \left(1 + \frac{8 l_o}{v_i} \frac{A_c}{A_p} \alpha n\right)^2 \quad . \tag{30}$$

The critical densities n_g, where $\Phi = 1$, were evaluated from Eq. (30) and compared with the corresponding experiments. Only if the experiments were performed at densities higher than or equal to n_g should the diffusion be taken into account. The following table represents the maximum density obtained in each experiment and the corresponding critical density. It is clearly seen that the diffusion can be neglected, in general. The diffusion could play a role, however, in the uppermost part of the curves of Figs. 5, 6, and 9. This would shift the experimental points above or to the left of the theoretical curves as the diffusion would contribute particles to the perturbed 'tube' of plasma. On the other hand, such a behaviour

is not observed. The end plate diffusion suggested by G. GRIEGER [9] also does not seem to be significant in the experiments described here.

Numerical Results

Experiment	Parameter	Fig.	Critical Density n_g for $\varphi \approx 1$	Experimental Density n_e
MOTLEY	$T_p = 2500^\circ K$	5	$n_g \approx 1.1 \times 10^{12}$ cm^{-3}	$n_e < 2.0 \times 10^{12}$ cm^{-3}
	$T_p = 2360^\circ K$	6	$\approx 1.7 \times 10^{12}$	$< 1.9 \times 10^{12}$
	$T_p = 2180^\circ K$	7	$\approx 2.1 \times 10^{12}$	$< 7.0 \times 10^{11}$
	$T_p = 1970^\circ K$	8	$\approx 2.2 \times 10^{12}$	$< 2.3 \times 10^{11}$
D'ANGELO v.GÖLER	Probe 'a'	9	$n_g \approx 3.0 \times 10^{11}$ cm^{-3}	$n_e < 1.0 \times 10^{12}$ cm^{-3}
	Probe 'b'	10	$\approx 1.3 \times 10^{12}$	$< 1.0 \times 10^{12}$
	Probe 'c'	11	$\approx 7.5 \times 10^{12}$	$< 8.0 \times 10^{11}$
ALMA II	Electron Sheath	12	$n_g \approx 5.0 \times 10^{12}$ cm^{-3}	$n_e < 4.0 \times 10^{10}$ cm^{-3}
	Ion Sheath	12	$\approx 1.0 \times 10^{12}$ cm^{-3}	$< 10^{12}$

Bibliography

1) L. Spitzer, Jr., "The Physics of Fully Ionized Gases", Intersci. Publ., New York (1962).

2) N. D'Angelo and N. Rynn, Phys. Fluids 4, 275, 1303 (1961).

3) S. v.Göler, Phys. Fluids 7, 463 (1964).

4) D. Eckhartt, G. Grieger, E. Guilino, M. Hashmi, Rep. MPI-PA-20/64.

5) R.W. Motley, Phys. Fluids 8, 205 (1965).

6) N. D'Angelo, S. v.Göler, Rep. MATT-314 (1964).

7) R.C. Knechtli, J.Y. Wada, Hughes Research Lab., Final Rep. Nonr 3501(00), June 1962.

8) H. Shelton, Phys. Rev. 107, 1553 (1957).

9) G. Grieger, Rep. MPI-PA-15/64.

10) N. D'Angelo, private communication.

Figure Captions

Fig. 1 Schematic diagram of a Q-machine showing A_c and A_p as well as imperturbed, perturbed, and 'effective' profiles.

Fig. 2 Perturbation region of a probe in a magnetic field. Plane (i) and cylindrical (ii) probes on the axis of a non-rotating plasma column, the direction of the magnetic field being perpendicular to the plane of the paper.

Fig. 3 Perturbation region of a probe for a rotating plasma in the magnetic field perpendicular to the plane of the paper. Cylindrical probe on (i) and off (ii) the axis of rotation.

Fig. 4 j_o/Φ_m vs. p_2/p_1.

Fig. 5-8 Comparison of theoretical n vs. j_o-curves with the experiments of MOTLEY.
(1) Equilibrium Theory
(2) Present Theory
(2a) Present Theory $T_p = 2450\,^{\circ}K$
(3) Equilibrium Theory $T_p = 2020\,^{\circ}K$
(4) Present Theory $T_p = 2020\,^{\circ}K$
The data marked x and ⊢—⊣ (see section 3.2) were taken with a probe midway between the hot end plates (102 cm apart). The circles represent probe data near the hot reflecting plate (plasma column 55 cm long).

Fig. 9-11 Comparison of theoretical n vs. j_o-curves with the experiment of D'ANGELO and v.GÖLER.
(1) Equilibrium Theory
(2) Present Theory
(2a) Present Theory $T_p = 2450\,^{\circ}K$
(3) Using in the present theory the empirical value of $A_p/A_c = 0.27$, as given in Ref. 6

Fig. 12 Comparison of calculated and experimental values of j_o as obtained by ECKHARTT et al.

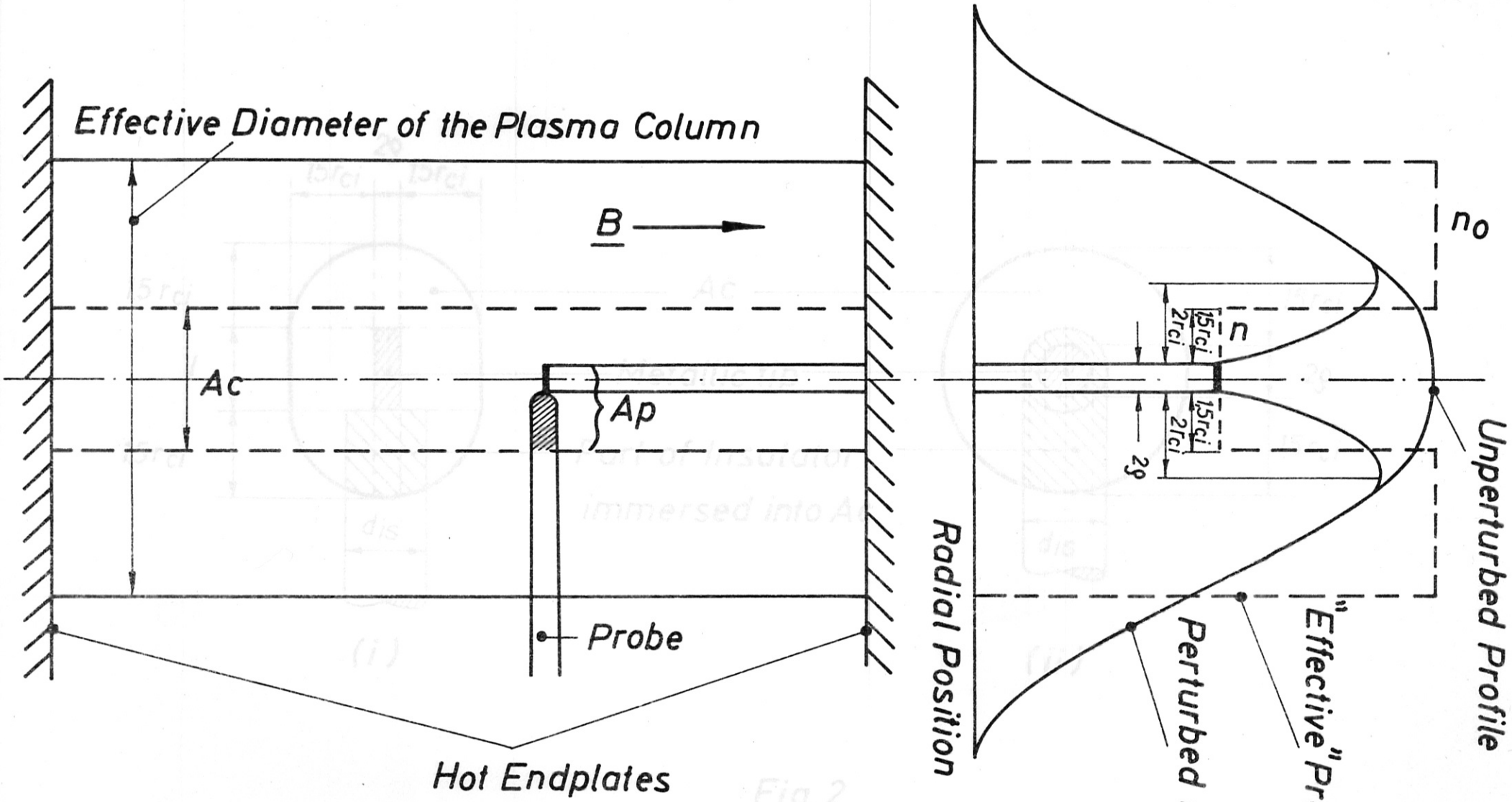
Effective Diameter of the Plasma Column
B
Ac
Ap
Probe
Hot Endplates
n
1.5rci
2rci
2g
n0
Unperturbed Profile
"Effective" Profile
Perturbed Profile
Radial Position

Fig.1

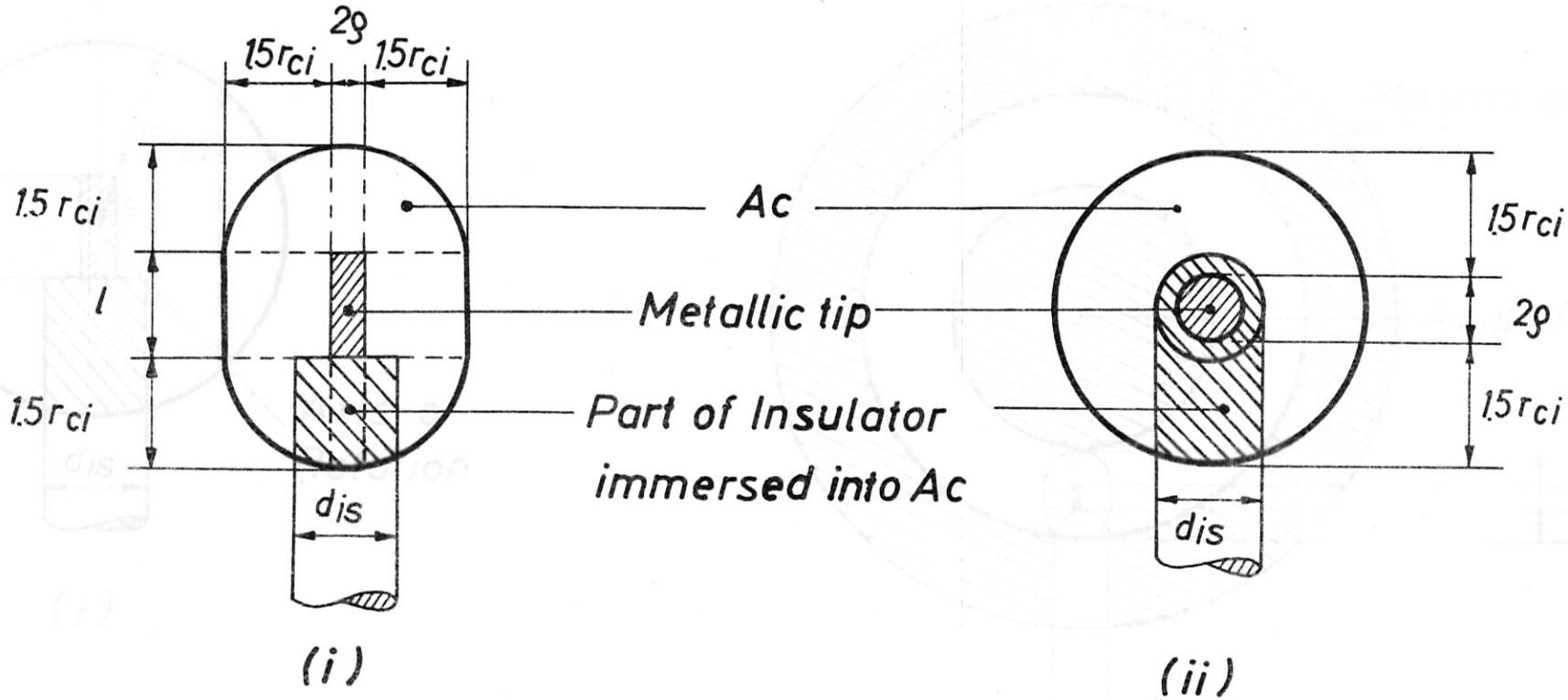
2ϱ
1.5rci
1.5rci
1.5 rci
l
1.5rci
dis
Ac
Metallic tip
Part of Insulator
immersed into Ac
1.5rci
2ϱ
1.5rci
dis
(i)
(ii)

Fig. 2

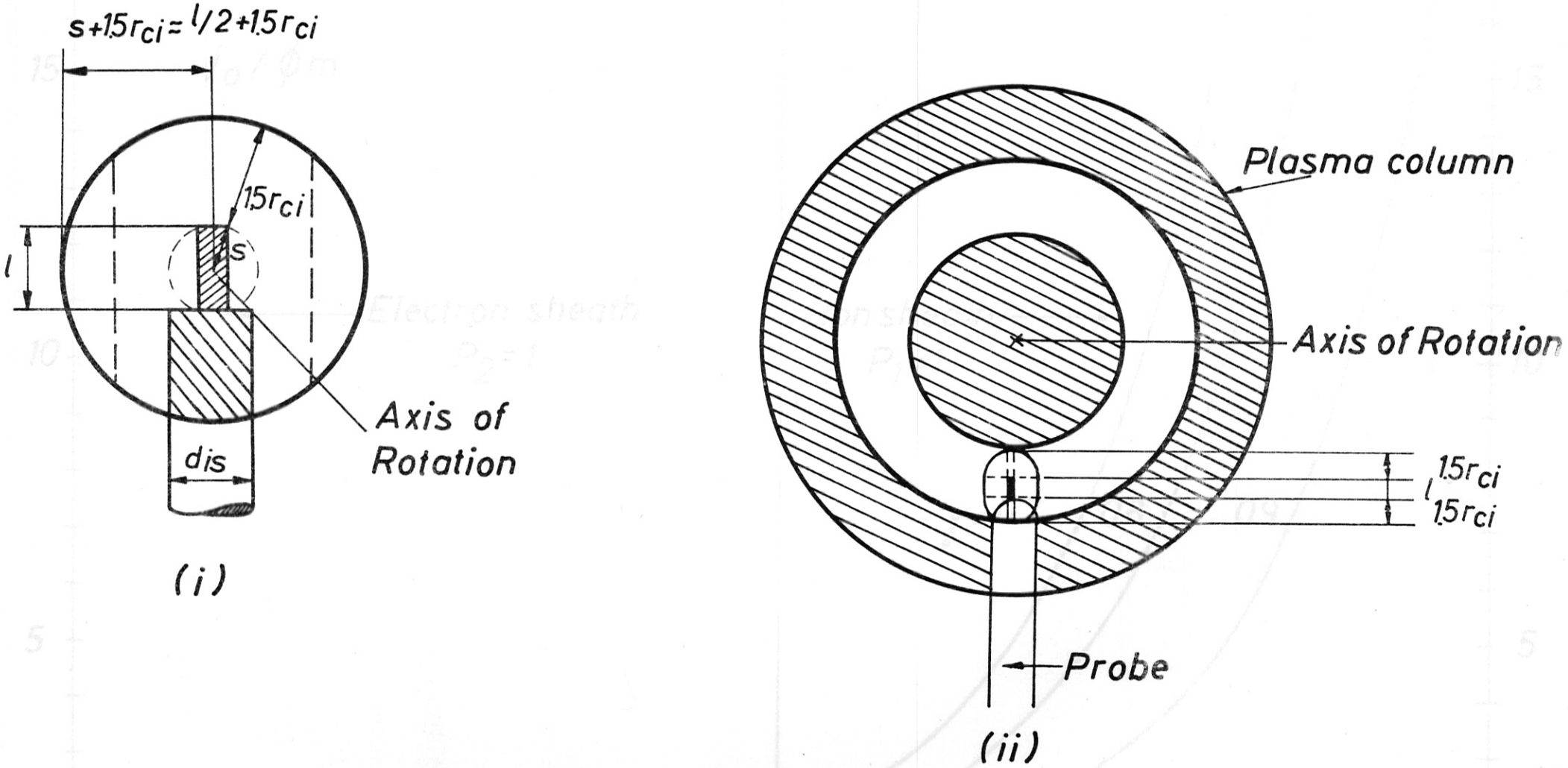
s+1.5rci = l/2+1.5rci
1.5rci
s
l
dis
Axis of Rotation
(i)
Plasma column
Axis of Rotation
1.5rci
l
1.5rci
Probe
(ii)

Fig.3

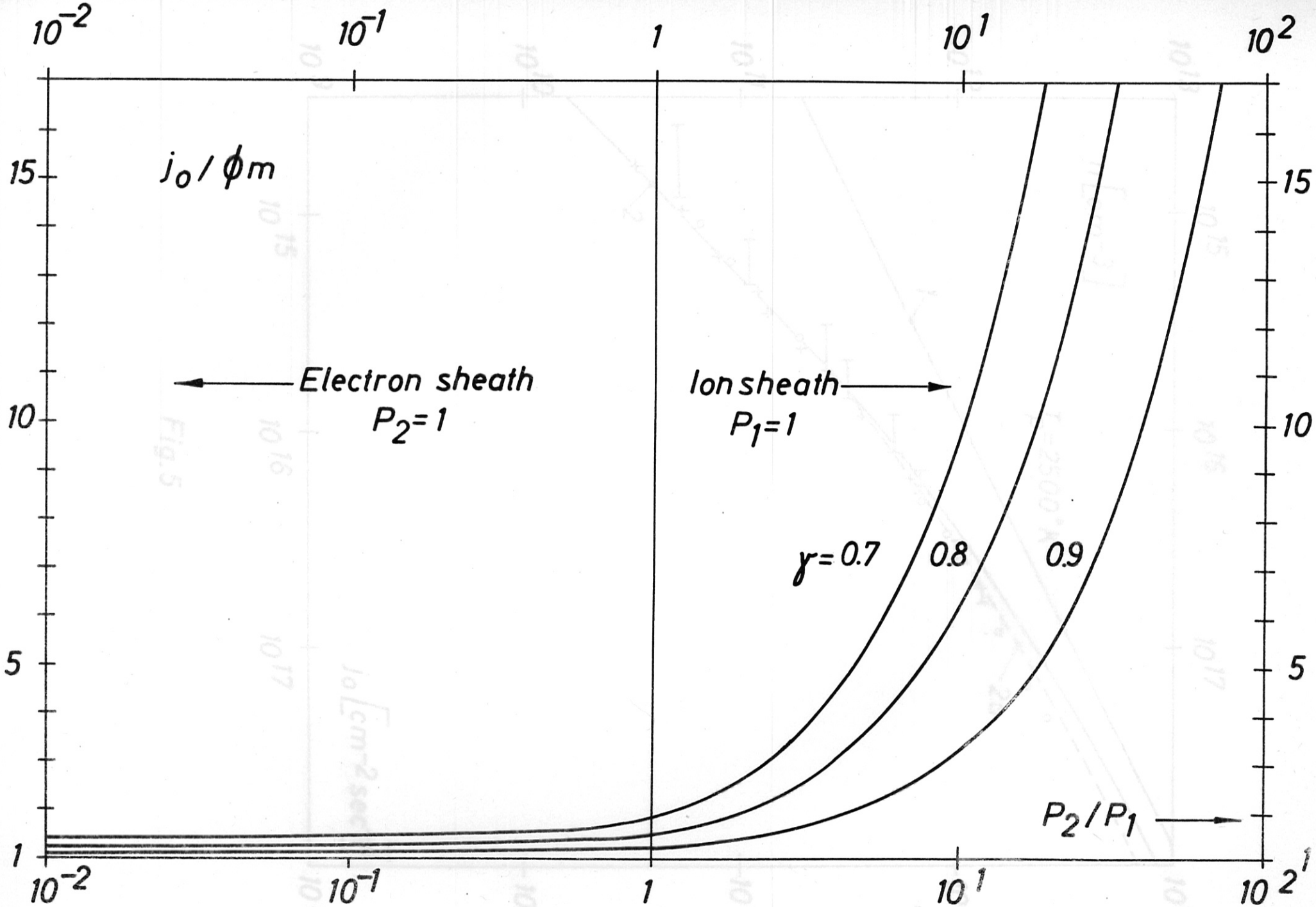
10^{-2}
10^{-1}
1
10^{1}
10^{2}
$j_o / \phi m$
15
10
5
1
Electron sheath
$P_2 = 1$
Ion sheath
$P_1 = 1$
$\gamma = 0.7$
0.8
0.9
P_2 / P_1
10^{2}

Fig.4

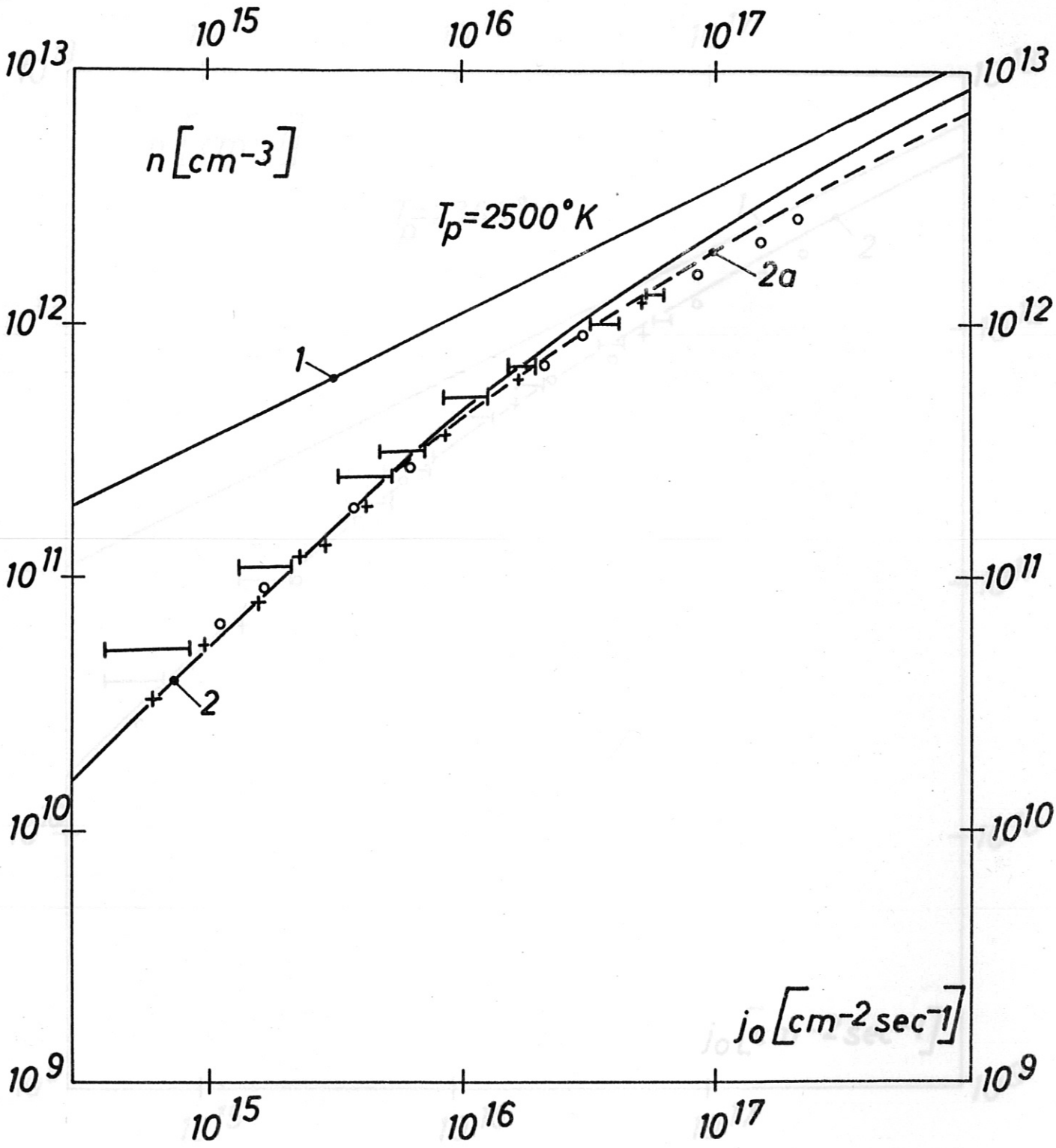
10^{15}
10^{16}
10^{17}
10^{13}
10^{12}
10^{11}
10^{10}
10^{9}
$n\,[cm^{-3}]$
$T_p = 2500°K$
1
2
2a
$j_o\,[cm^{-2}sec^{-1}]$

Fig. 5

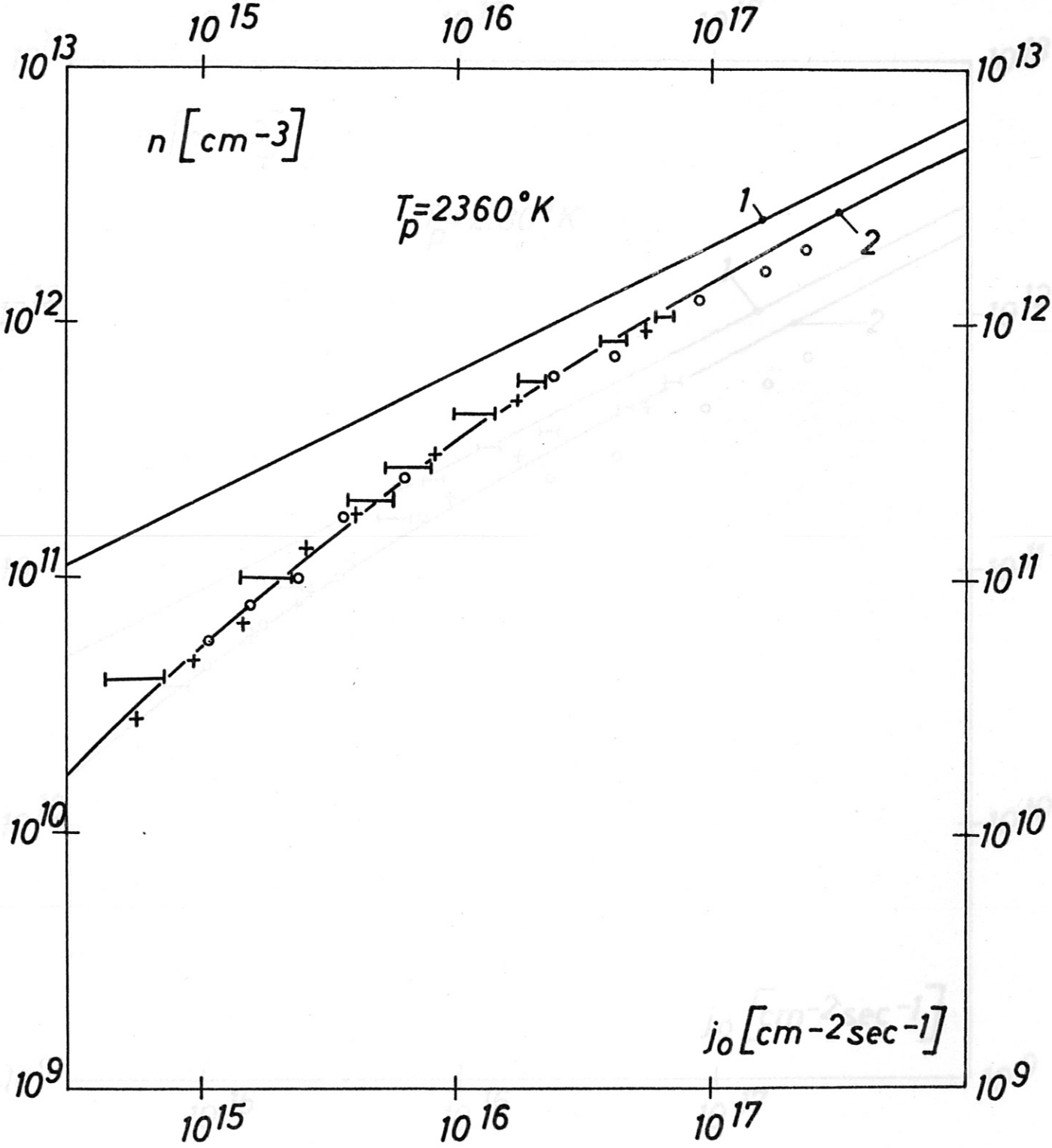
10^{15}
10^{16}
10^{17}
10^{13}
$n\ [cm^{-3}]$
$T_p = 2360°K$
1
2
10^{12}
10^{11}
10^{10}
10^{9}
$j_o\ [cm^{-2}sec^{-1}]$

Fig. 6

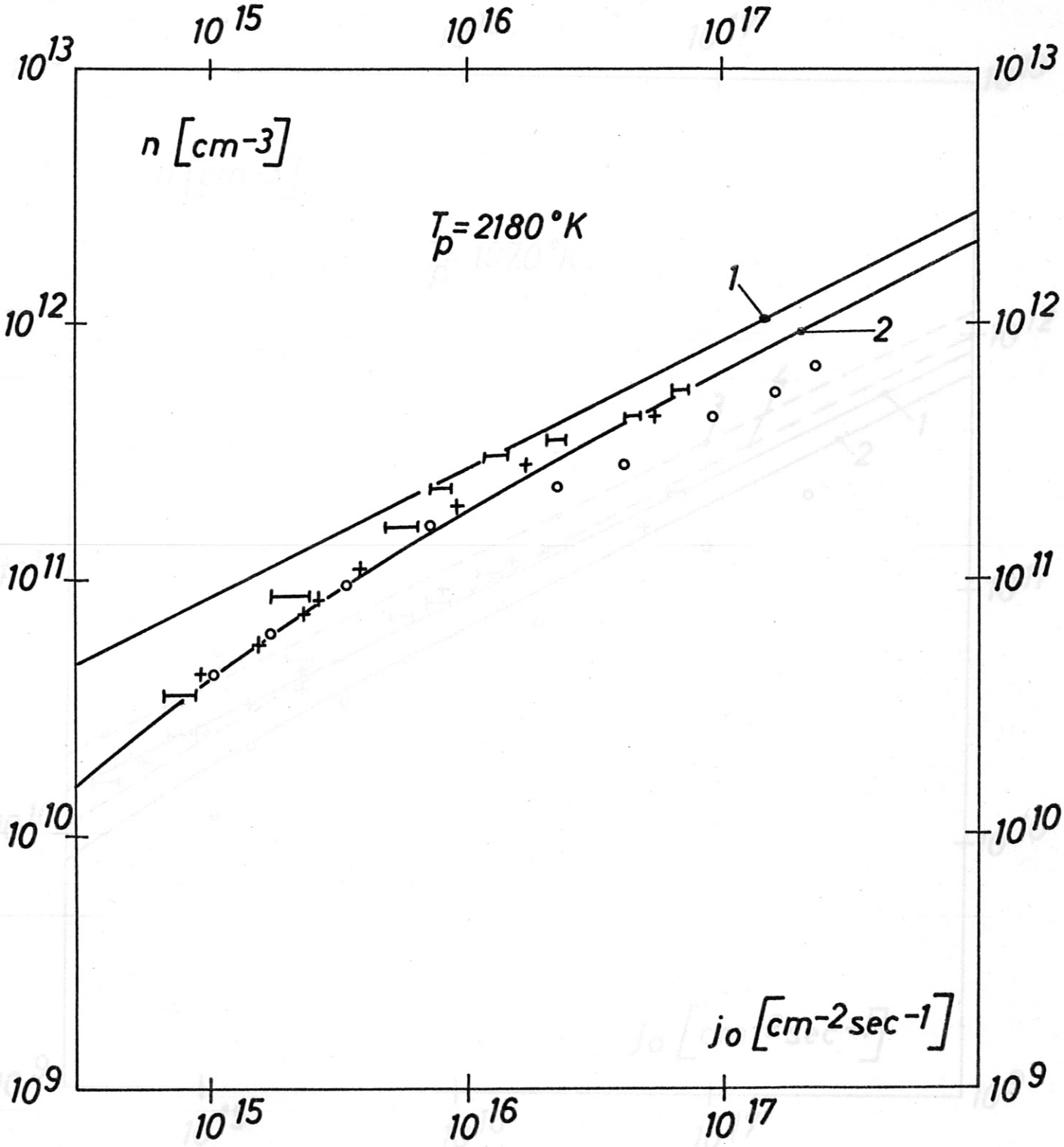
10^{15}
10^{16}
10^{17}
10^{13}
10^{13}
$n\ [cm^{-3}]$
$T_p = 2180\,°K$
1
2
10^{12}
10^{12}
10^{11}
10^{11}
10^{10}
10^{10}
$j_o\ [cm^{-2}sec^{-1}]$
10^{9}
10^{9}
10^{15}
10^{16}
10^{17}

Fig. 7

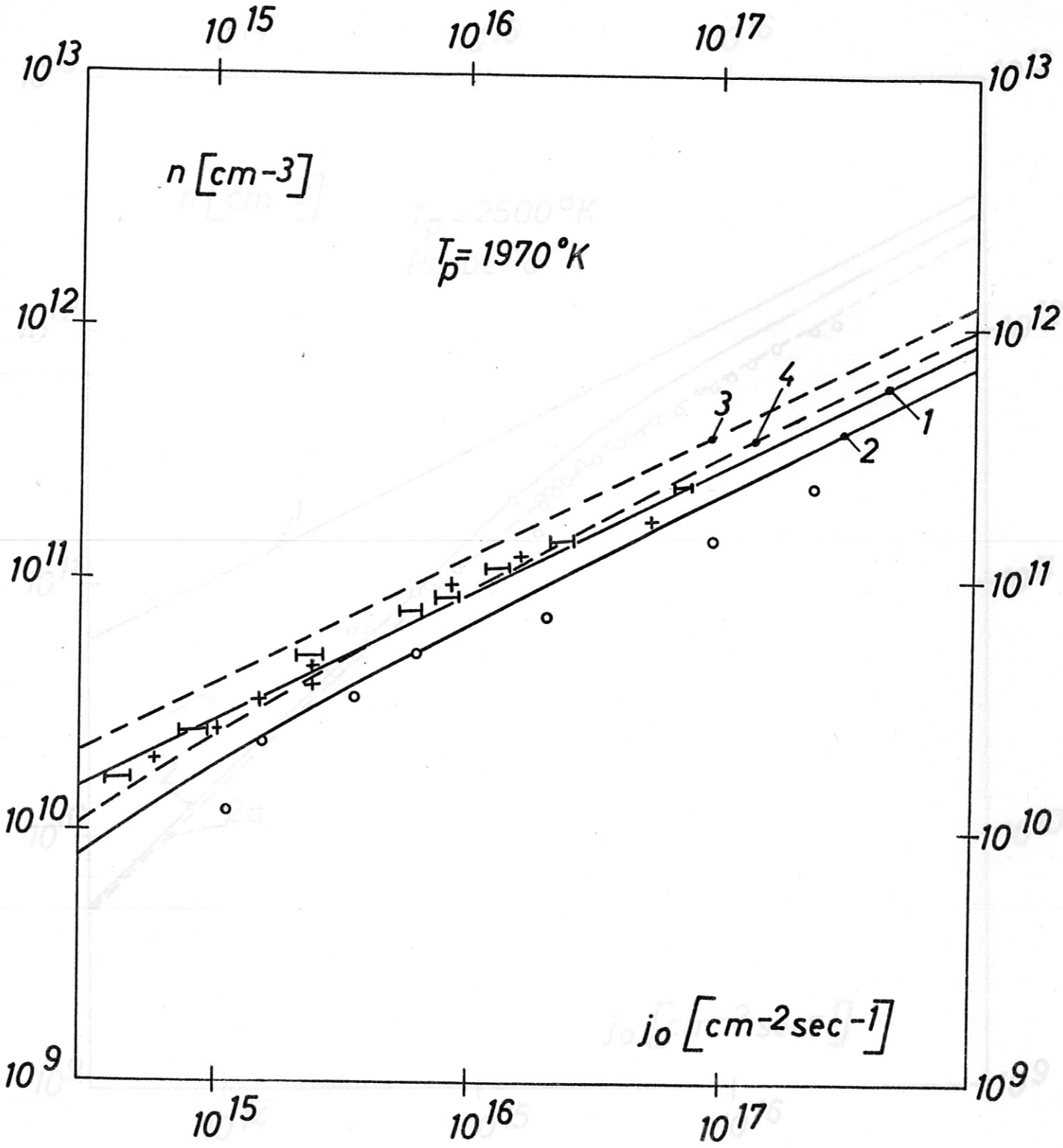
10^{15}
10^{16}
10^{17}
10^{13}
10^{13}
n [cm-3]
T_p= 1970 °K
10^{12}
10^{12}
1
2
3
4
10^{11}
10^{11}
10^{10}
10^{10}
j_o [cm-2sec-1]
10^{9}
10^{9}
10^{15}
10^{16}
10^{17}

Fig. 8

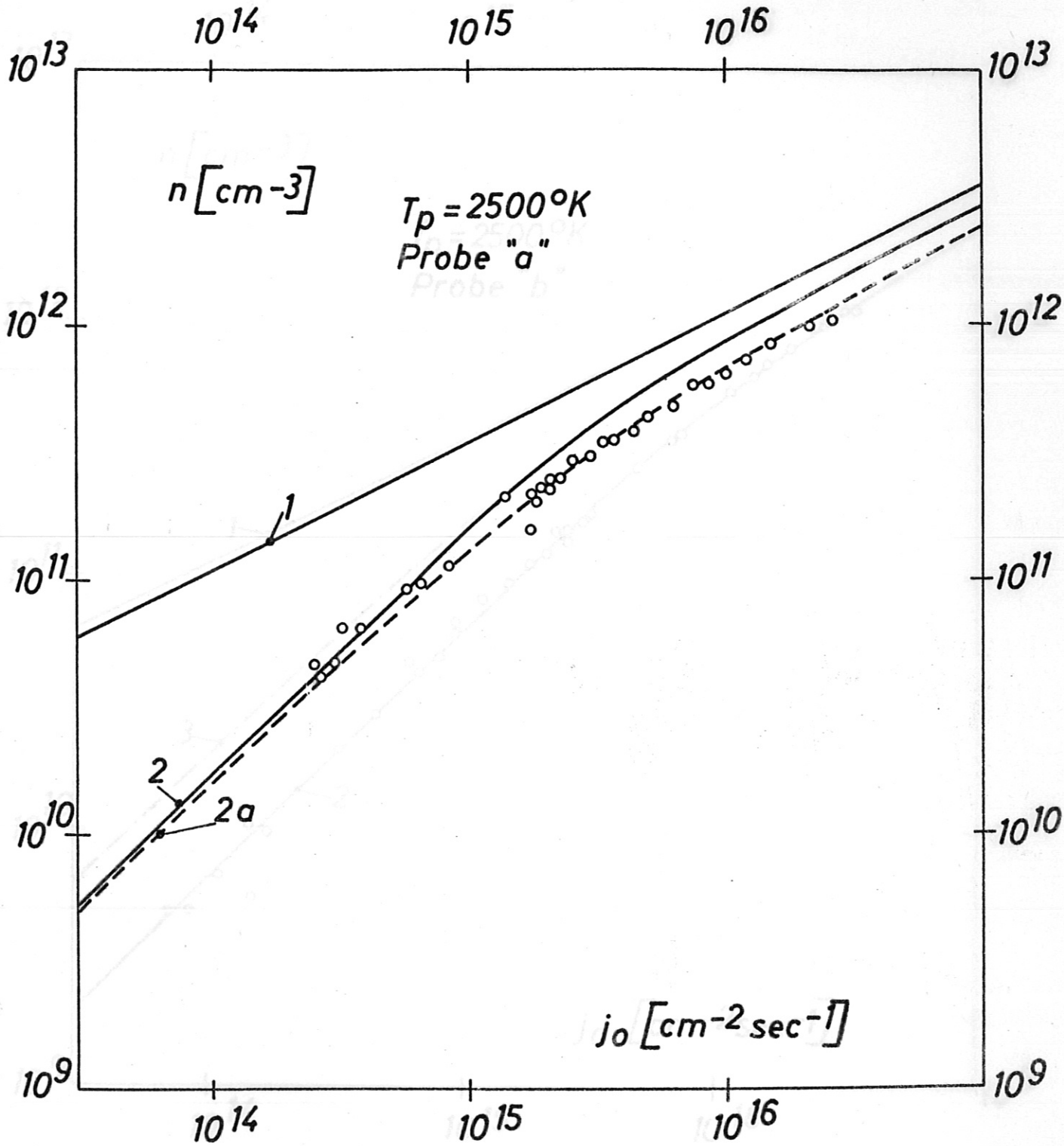
10^{14}
10^{15}
10^{16}
10^{13}
10^{13}
$n\,[cm^{-3}]$
$T_p = 2500°K$
Probe "a"
10^{12}
10^{12}
1
10^{11}
10^{11}
2
2a
10^{10}
10^{10}
$j_o\,[cm^{-2}\,sec^{-1}]$
10^{9}
10^{9}
10^{14}
10^{15}
10^{16}

Fig.9

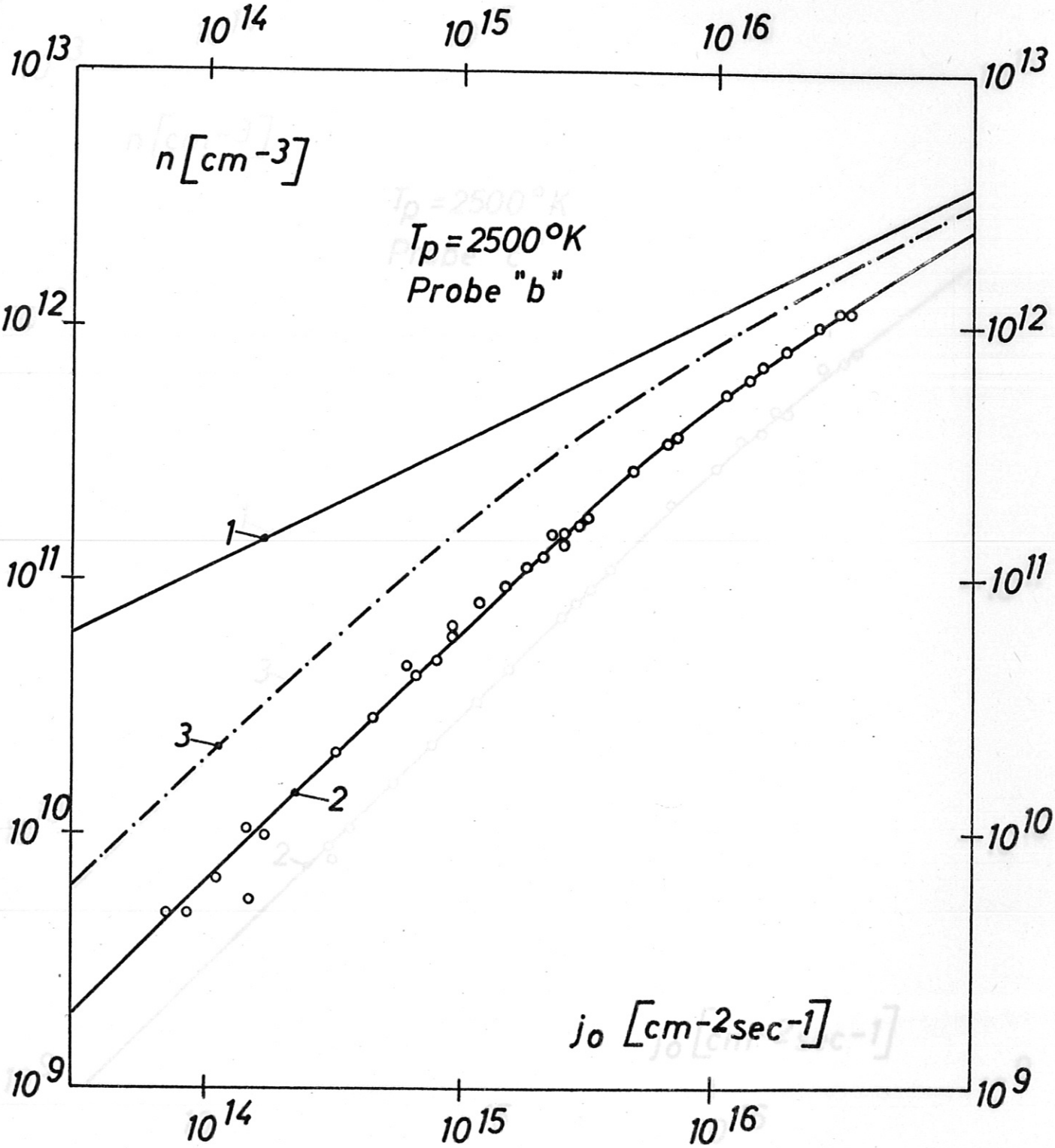
10^{13}
10^{14}
10^{15}
10^{16}
$n\,[cm^{-3}]$
$T_p = 2500\,^{\circ}K$
Probe "b"
10^{12}
10^{11}
10^{10}
10^{9}
1
2
3
$j_o\,[cm^{-2}sec^{-1}]$

Fig.10

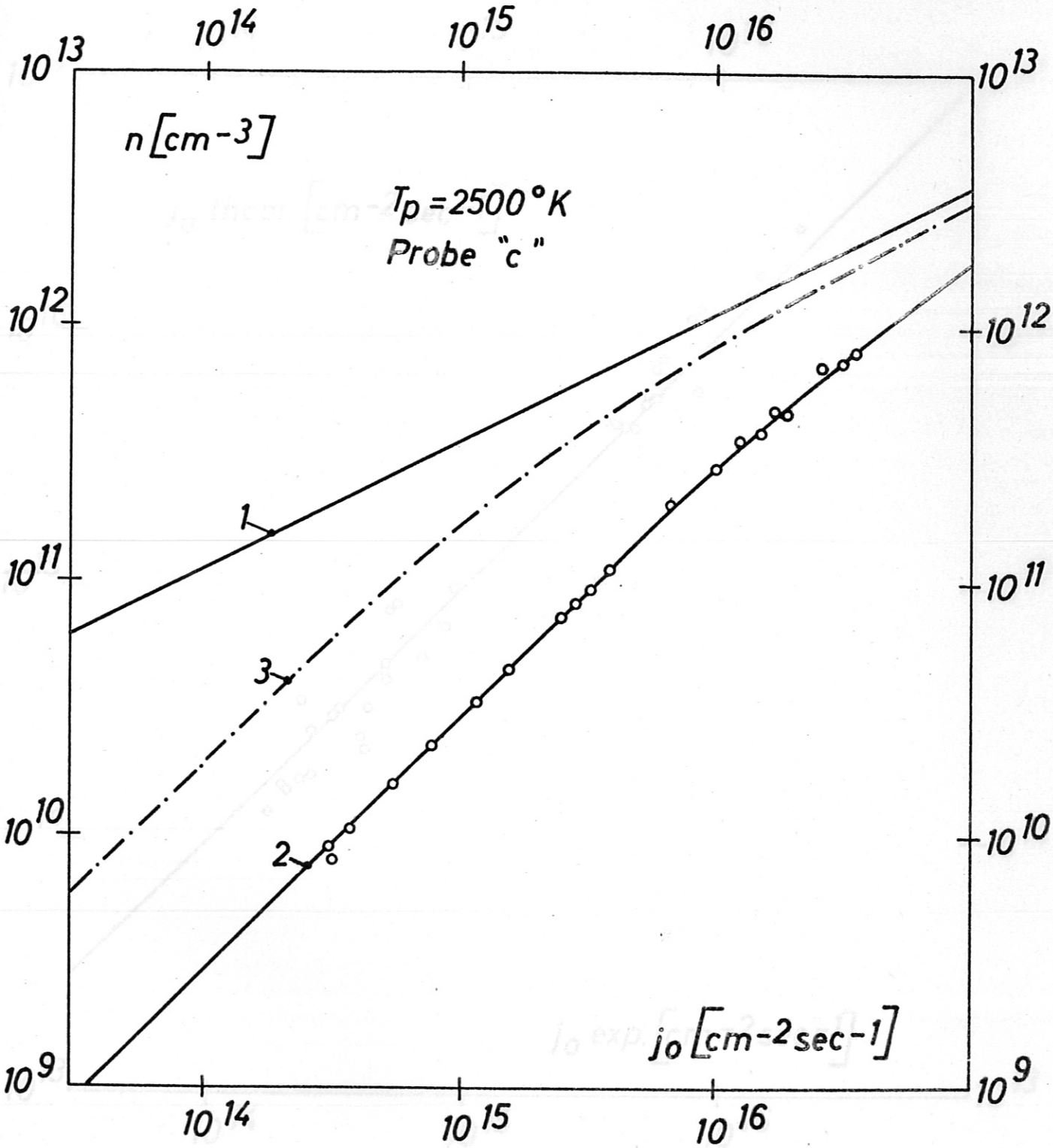
10^{13}
10^{14}
10^{15}
10^{16}
n [cm-3]
$T_p = 2500°K$
Probe "c"
10^{12}
10^{11}
10^{10}
10^{9}
1
2
3
j_o [cm-2sec-1]

Fig. 11

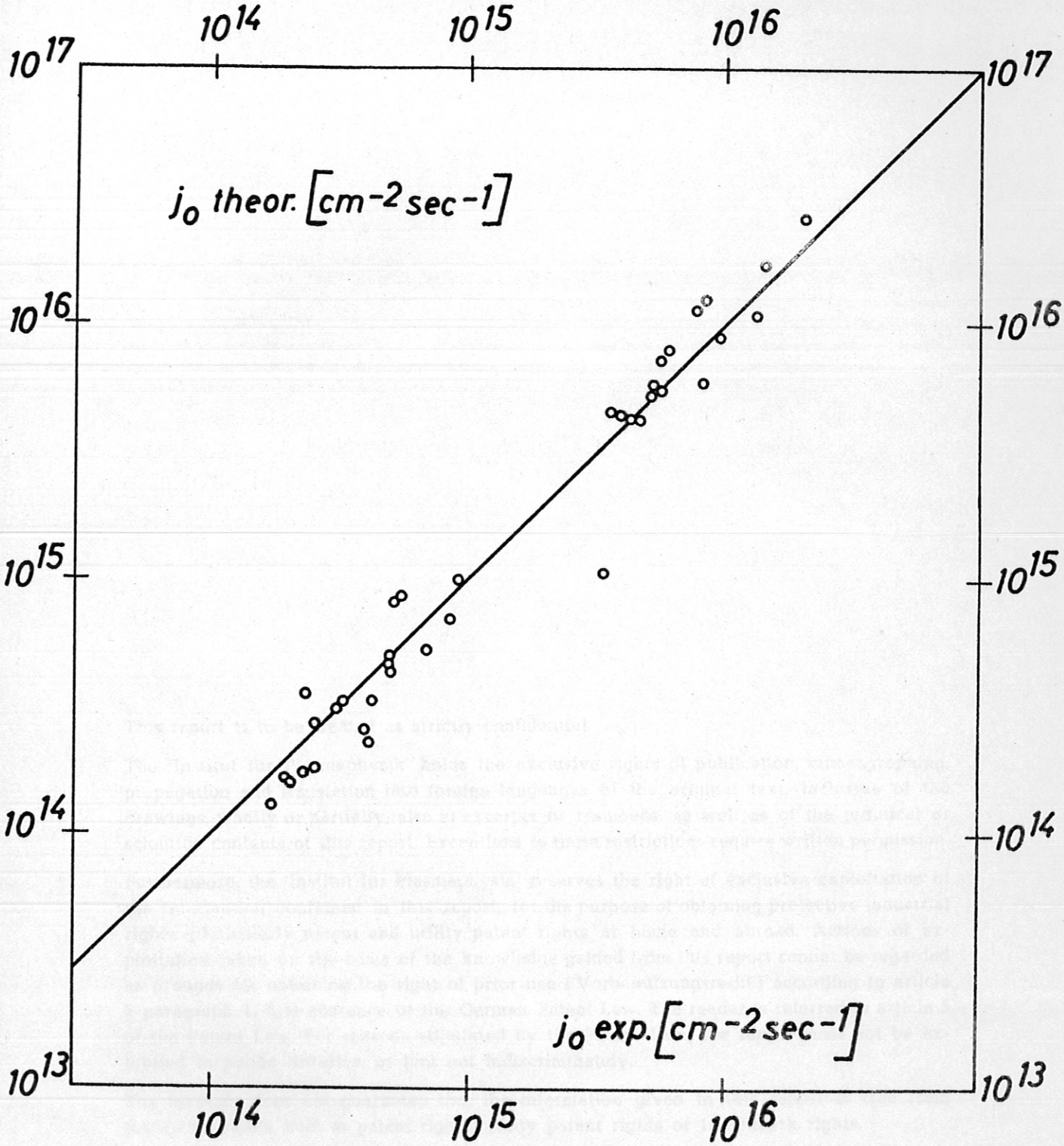
10^{14}
10^{15}
10^{16}
10^{17}
j_o theor. [cm^{-2}sec^{-1}]
10^{16}
10^{15}
10^{14}
10^{13}
j_o exp. [cm^{-2}sec^{-1}]
10^{17}
10^{16}
10^{15}
10^{14}
10^{13}
10^{14}
10^{15}
10^{16}

Fig.12